



Monitoring Land Cover Changes in Tehran City over 5 years (2018 to 2022) using Remote Sensing based Spatial Information

Sara Vahidi^a, Vahid Hatamzadeh^{a++*}, Paniz Nouri^a
and Afshin Afshin Far^a

^a Islamic Azad University, Tehran, Iran.

Author's contribution

This work was carried out in collaboration among all authors. All authors read and approved the final manuscript.

Article Information

DOI: 10.9734/AJEE/2023/v20i3440

Open Peer Review History:

This journal follows the Advanced Open Peer Review policy. Identity of the Reviewers, Editor(s) and additional Reviewers, peer review comments, different versions of the manuscript, comments of the editors, etc are available here: <https://www.sdiarticle5.com/review-history/97756>

Original Research Article

Received: 25/01/2023
Accepted: 27/03/2023
Published: 04/04/2023

ABSTRACT

Rapid economic growth has increased the speed of resource changes and many of these changes have rapid and harmful effects. Natural environment such as agriculture, forest, water resources, value Cultural things such as historical landscape and health Humans have put Land use changes directly. It changes the resources of the earth, which affects the temperature and humidity causes changes in the climate and weather of the region as well. It reduces cultivated areas [1]. Considering that one of the main prerequisites for the optimal use of land, obtaining information. One of the patterns of land use over time is map design. Related specializations are one of the most important goals in management. It is considered natural resource [2]. In recent years, preparing land use maps by digital classification of remote sensing data have been advertised as appropriate alternative for using this type of maps. Remote sensing is a modern and useful technique in updating land use maps and detecting new changes. In this research ArcGIS pro used for classification that is one of

⁺⁺ Student;

*Corresponding author: E-mail: vahid4251@yahoo.com;

the most accurate and updated software for remote sensing's process for detecting 4 main type of classes in Tehran city in IRAN. standard accuracy in satellite image processing is important criteria in this study with standard kappa coefficient accuracy, and overall accuracy of data calculated for each maps, by considering 4 essential classes in a major city and converted to maps of changes in linear regression concluded that build-up class have a significant slope increase 3422/3 (hectares), plant class is improving during the study period as 2821/71 (hectares) but these increment are inhomogeneous, water class has sharp drop as 443.52 (hectares), Then the most of decrement is for the barren area which named soil class as 5800.48 (hectares). Part of accuracy in this research depends on severity of the numbers of test samples which given for classification that are more than 5000 pixels to assessment reliable results. According to the standards of kappa coefficient that provided in USGS earth data site all off maps are acceptable.

Keywords: Remote sensing (RS); satellite images; land cover-land change; ArcGIS Pro; classification; sentinel 3.

1. INTRODUCTION

In the last decades urban development caused increasing the land uses changes these changes can duo several reason such as economic, political and cultural but Construction and Urban development is the most important activity that has changed the land cover. Knowledge of the type and percentage of different uses is necessary for the recognition and management of natural and environmental resources at the level of watersheds and other work units. The increment of pressure on the natural areas caused by the growth of the population and unprincipled exploitation and changes of use have caused the destruction of the ecosystems. In fact, revealing changes is one of the main factors in investigating the relationship between human activities and the environment. Land use emphasizes the social aspect of using pattern. In other words, land use is the output of activities that humans perform according to their economic and social needs. In this way, land use is the process of transforming a natural ecosystem into a social ecosystem, which is based on the functioning of nature, economy, and society. Since changes in land use are considered as irreversible changes, access to update information and awareness of these changes are key factors in the management and planning in organizations; this will be possible by detecting land use changes. Using common and traditional methods of land measurement requires a lot of time and cost, and it is not possible to do it even in some inaccessible areas. The use of satellite images due to its special features such as wide visibility and low cost, using different parts of the electromagnetic spectrum to record the characteristics of phenomena, short return period, the possibility of automatic analysis, faster investigation and also providing the

possibility of monitoring the area, have a particular importance [3]. Remote sensing data with features such as repeated imaging in short time intervals, the vastness of the land cover surface taken by the sensors, suitable spectral and spatial resolution of the data provide a suitable tool for investigating land cover changes. Today, progress in remote sensing techniques has provided considerable opportunities and successes to observe and manage the rapid growth of cities. In the field of determining land use and land cover, many studies have been conducted in the world and the use of satellite data such as Landsat, Spot and IRS in preparing maps has been approved by many experts. Several researches in this field have done. Alijenaid et, al detected land use and land cover using GIS and remote sensing technique in Bahrain over 1986-2020. they used multi spectral and multi temporal satellite images. They classified images using maximum likelihood algorithm to generate the seven LULC maps [4]. In 2022, Nima Karimi and colleagues used satellite images to identify the areas of landfill without permission in the Saskatchewan region, located north of Saskatoon in Canada. For this research, they used Landsat 8 images to produce land surface temperature and MSAVI vegetation index and vector data of railways and highways. In this research, by weighting the layers and using the fuzzy method, unlicensed landfill areas were discovered and favorable areas for landfilling were also located [5]. In 2022, Ike Felix et al used remote sensing and GIS techniques to identify suitable sites for solid waste disposal in the city of Aba, located in the southeast of Nigeria. For this research, they used Landsat 8 image, SRTM data, GPS coordinates, geological map, soil map, and land use map to produce a suitability map of areas for landfilling.

The results showed that the most suitable potential areas for solid waste landfill sites are located about 5000 meters west of Ariaria market and 10000 meters southeast of Umo Mba in Aba city [6]. Yang et al. This map generated with overall accuracy about 85% and overall kappa coefficient between 87% to 95%. They found out the increment in the built-up area was dominant over the last 3 decades [7]. Clarifying and predicting the changes in land covering and urban growth are keys to present the holistic and principled views on more efficient management of environmental resources, protection of suburban lands and adoption of long-term policies to minimize the impacts of urban development on the environment and even to appreciate the potential impacts on socioeconomic resources as well as people [8]. Kumar and Singh studied on geospatial application in land use land cover detection in developed region. They used Landsat 2,3,5,7 and 8 image for the years 1975-2020 for central Haryana, India. They used unsupervised classification to classify the images in eight classes. The year 1975 considered as the base year for change detection analysis. Their results showed an increasing trend for the land use classes of built-up, water body and agricultural land without water logging between 1975 and 2020. Also land use classes of agriculture with water logging, open water logged area vegetation and fallow land decreased during the same period. The most achievement of their paper is the human activity had a great impact on land-cover land-changes in the developed area [9]. Guanyao Xie and Niculescu studied on monitoring of land cover land changes in Crozon Peninsula. They used high-resolution imagery to evaluate multi annual change detection using support vector machine (SVM) and random forest (RF) and convolutional neural network (CNN) with Spot5 and Sentinel2 data from 2007 and 2018. In their research the CNN had significantly high accuracy than the SVM and RF up to 90% also inclusion of the CNN significantly improved the classification performance (5-10% increase in the overall accuracy) compared with the SVM and RF classifiers [10]. Wang et al. conducted a study in a coastal area of Dongguan city China using Spot5 images acquired in 2005 and 2010. In this study scale parameter and location of the local maximum of a weighted local variance was proposed to determine the scale selection problem when segmenting images constrained by LCLU for detection changes [11]. Gun et al. 2020 studied a CD and classification algorithm for urban expansion

processes in Tianjin (coastal city in China) based on Landsat time series from 1985 to 2019. They applied the C-factor approach with the Ross Thick-LiSparse-R model to correct the bidirectional reflectance distribution function (BRDF) effect for each Landsat image and calculated a spatial line density feature to improve the CD and the classification [12]. In 2019, Hisham Abdul Mansef et al. used the combination of remote sensing, geographic information system and hierarchical analysis process to select a hazardous waste landfill site. The area studied in this research was the hazardous industrial wastes of the Suez Canal in Egypt. To implement the AHP model, they used the parameters set in the Basel Convention on Hazardous Waste, which was established in 1992. These parameters included social, economic, environmental, geological, hydrological and geomorphological parameters. Using the AHP method and the mentioned parameters, two suitable places for hazardous waste disposal were identified (Mansef, 2019). There is no updated study about Tehran metropolis classification with ArcGIS Pro and maximum likelihood classification method and using linear regression to predict future years' changes with high spatial accuracy using Sentinel satellite images. Because of importance of Tehran as a crowded city this issue has been assisted to with determining the process of changes, correct decisions for prevention to adopt changes in usage and comprehensive management at the level of this basin be made [13].

2. STUDY AREA

This paper studied on the change detection in Tehran over the 2018-2020. Tehran city is located at 51°6' to 51° 38' east longitude and 35°34' to 35°51' north latitude and its height from the (MSL) is between 1800 meters in the north and 1200 meters in the center and 1050 meters in the south is variable. This city has an area of about 730 square kilometers, Tehran is spread between mountain and the desert and on the southern slopes of the Alborz mountain range. It is surrounded from the south by the mountains of Ray and Bibi Shahrabano and the flat plains of Shahriar and Varamin, and from the north by the mountains. The amount of annual rainfall in Tehran is mostly low and is 245.8 mm. The highest temperature in Tehran was 43 degrees Celsius and the lowest temperature was -15 degrees Celsius [14]. Fig. 1 shows the location of the study area:

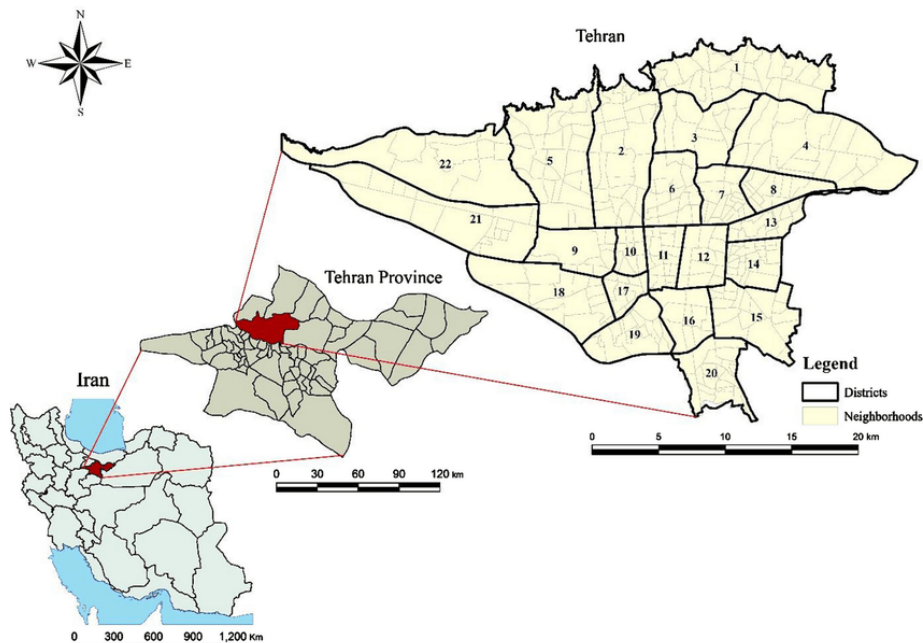


Fig. 1. Location map of study area [15]

3. METHODOLOGY

In this study sentinel 3 satellite images for 5 continuous years 2018 to 2022 downloaded from Copernicus open access earth data site, for Implementation of correction ENVI5.6 had been done and then remote sensing software ArcGIS Pro sentinel satellite image processing was used. During the image process geometric, radiometric and atmospheric correction have been done. ArcGIS Pro is a modern, fast, and powerful GIS for analyzing your data [16]. ArcGIS Pro is a full-featured professional desktop GIS application from Esri. With ArcGIS Pro, you can explore, visualize, and analyze data; create 2D maps and 3D scenes; and share your work to ArcGIS Online or your ArcGIS Enterprise portal. The sections below introduce the sign-in process, the start page, ArcGIS Pro projects, and the user interface. This gives the power to examine relationships, test predictions, and ultimately make better decisions [17]. Classification of satellite images is conventionally divided into supervised and unsupervised methods. Supervised methods need basic information such as feature class and detector samples of each class, while unsupervised methods are automatic and by depended on pixel's value make decision about classification. The maximum likelihood algorithm is one of the parametric methods of supervised classification. This method is one of the most famous classification methods based on pixels. It is

common to use a threshold limit in this method, if a threshold limit is used, some pixels will be unmatched, determining the threshold value is very important based on the type of class and the amount of their spectral overlap the maximum likelihood algorithm using the multidimensional normal distribution formula makes decision level in a quadratic form and levels will have a parabolic shape. The cofactor matrix that in addition to average vector used in this algorithm makes more features of the data to be used, thus increasing the classification accuracy [18]. In this paper maximum likelihood algorithm used for image classification. The accuracy of the prepared thematic maps increases according to the number of test samples, and in this study we achieved good accuracy with a number of more than 5000 sample pixels.

3.1 Sentinel-3

The main goal of the Sentinel-3 (OLCI) mission is to measure the topography of the ocean surface, the surface temperature of the earth and the sea, to measure the color of the surface of the earth and the ocean with the accuracy required for forecasting systems of the state of the oceans and environmental and climate monitoring [19]. OLCI observation is performed simultaneously in 21 spectral bands, listed in the table below, each of these bands is programmable in position (htt2) sentinel-3 images have been used in this paper for better spatial resolution and improvement of productions.

Table 1. OLCI Band characteristics [20]

| | | | |
|------|---------|------|------------------------------------------------------------------------------------------------------------|
| Oa01 | 400 | 15 | Aerosol correction, improved water constituent retrieval |
| Oa02 | 412.5 | 10 | Yellow substance and detrital pigments (turbidity) |
| Oa03 | 442.5 | 10 | Chlorophyll absorption maximum, biogeochemistry, vegetation |
| Oa04 | 490 | 10 | High Chlorophyll, |
| Oa05 | 510 | 10 | Chlorophyll, sediment, turbidity, red tide |
| Oa06 | 560 | 10 | Chlorophyll reference (Chlorophyll minimum) |
| Oa07 | 620 | 10 | Sediment loading |
| Oa08 | 665 | 10 | Chlorophyll (2nd Chlorophyll absorption maximum), sediment, yellow substance/vegetation |
| Oa09 | 673.75 | 7.5 | For improved fluorescence retrieval and to better account for smile together with the bands 665 and 680 nm |
| Oa10 | 681.25 | 7.5 | Chlorophyll fluorescence peak, red edge |
| Oa11 | 708.75 | 10 | Chlorophyll fluorescence baseline, red edge transition |
| Oa12 | 753.75 | 7.5 | O2 absorption/clouds, vegetation |
| Oa13 | 761.25 | 2.5 | O2 absorption band/aerosol correction. |
| Oa14 | 764.375 | 3.75 | Atmospheric correction |
| Oa15 | 767.5 | 2.5 | O2A used for cloud top pressure, fluorescence over land |
| Oa16 | 778.75 | 15 | Atmos. corr./aerosol corr. |
| Oa17 | 865 | 20 | Atmospheric correction/aerosol correction, clouds, pixel co-registration |
| Oa18 | 885 | 10 | Water vapor absorption reference band. Common reference band with SLSTR instrument. Vegetation monitoring |
| Oa19 | 900 | 10 | Water vapor absorption/vegetation monitoring (maximum reflectance) |
| Oa20 | 940 | 20 | Water vapor absorption, Atmospheric correction/aerosol correction |
| Oa21 | 1020 | 40 | Atmospheric correction/aerosol correction |

3.2 Improving Spatial Resolution

In this process the data integration process can be applied to improve the quality and quantity of the images. There are various methods of performing fusion, which include:

- Methods based on cell processing
- Methods based on complications
- Statistical methods

The results of merging data have more spatial resolution, appropriate accuracy and have a valuable visual quality for interpretation also it can provide the possibility of targeted processing of multi-temporal, multi-sensor and multi-spectral image.

3.3 Accuracy Analysis

After classifying the images, using educational samples that are not involved in the classification process, the validation of the unclassified image is evaluated. ArcGIS methods for spatial information are new technique with high resolution and High reliability.

3.3.1 Producer accuracy

The producer accuracy expresses the probability that a pixel in the classified image is located in

the same class on the ground and computed as below:

$$\text{Accuracy} = \frac{c_{aa}}{c_a} \times 100\% \quad (1)$$

Where, c_{aa} = element at position a^{th} Row and a^{th} column and c_a =column sums

The minimum acceptable accuracy for a class is 90% [21]

3.3.2 User accuracy

The user accuracy expresses the probability that a certain class on the ground is placed in the same class on the classified image as below:

$$\text{User accuracy} = \frac{c_{ii}}{c_i} \times 100\% \quad (2)$$

Where, c_{ii} is =element at position a^{th} row and a^{th} column and c_i =column sums and c_i = row sums.

3.3.3 Overall accuracy

The overall accuracy is obtained from the sum of the main diameter's elements of the error matrix divided by the total number of pixels according to the following equation:

$$\text{Overall Accuracy} = \frac{\sum_{a=1}^u c_{aa}}{Q} \times 100 \quad (3)$$

Where Q and U is the total number of pixels and classes respectively. The minimum acceptable overall accuracy is 85% [21].

3.3.4 Kappa coefficient

The kappa coefficient K is a second measure of classification accuracy which incorporates the off-diagonal element as well as diagonal term to give a more robust assessment of accuracy than overall accuracy it is computed as: [3].

$$k = \frac{\sum_{a=1}^u \frac{c_{aa}}{Q} - \sum_{a=1}^u \frac{c_a c_a}{Q^2}}{1 - \sum_{a=1}^u \frac{c_a c_a}{Q^2}} \quad (4)$$

Where c_a =row sums.

3.4 Linear Regression

One of the methods of regression analysis. Regression is a type of statistical model for predicting one variable from one or more other variables. Linear regression is a type of linear predictor function in which the dependent variable - the variable to be predicted - is predicted as a linear combination of independent variables, which means that each of the independent variables is multiplied by the coefficient obtained for that variable in the estimation process. Will be the final answer will be the sum of the products plus a constant value, which is also obtained in the estimation process [15].

Simple linear regression measures the effect of an independent variable on a dependent variable and measures the correlation between them [22]. For simple regression analysis with N point, x_i independent variable and β_0, β_1 are linear coefficients:

$$y_i = \beta_0 + \beta_1 x_i + e_i \quad i=1, \dots, N \quad (5)$$

e_i Demonstrates error and i is the number of observation (x_i, y_i) model can be simulated by numbers of these points, common method to obtain the parameters is the least squares method. In this method, the parameters are obtained by minimizing the sum of squared errors:

$$SSE = \sum_{i=1}^N e_i^2 \quad (6)$$

$$\beta_1^\wedge = \frac{\sum_{i=1}^N (x_i - \bar{x})(y_i - \bar{y})}{\sum_{i=1}^N (x_i - \bar{x})^2} \quad (7)$$

That 6 and 7 are equal.

3.5 Maximum Likelihood Classification

One of the most accurate and widely used methods among the various supervised classification methods is the maximum likelihood method. This method evaluates the variance and covariance of different classes. In the maximum likelihood method, it is assumed that all educational regions have a normal distribution function. After evaluating the probabilities in each class, the pixels are assigned to the classes that have the most similarity, and if the probability values are lower than the threshold, they introduce as unclassified pixels [23,24].

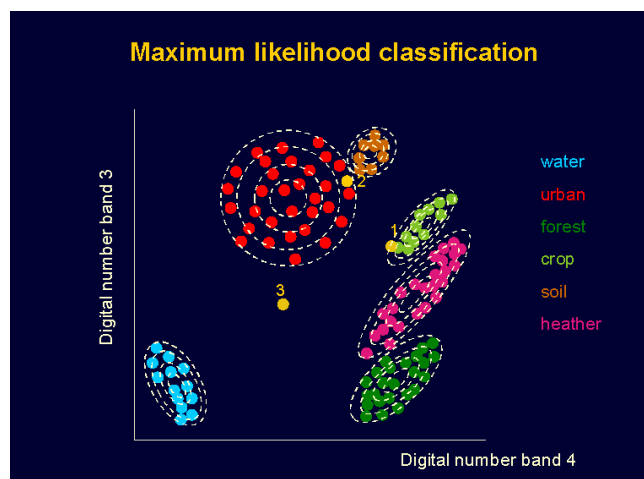


Fig. 2. Maximum likelihood classification [23]

4. RESULTS AND DISCUSSION

After process, corrections and classify the satellite images. This procedure done by ENVI and ArcGIS Pro software and five maps are generated about land use change in Tehran during 2018-2022 as below. These maps divided to 4 classes and then following prepared charts and tables which Total area of Tehran metropolis validated by urban management of Municipality in each year are clarifying the results.

Total amount of kilometers are checked with the governmental statistics data of Municipality and urban development (www.tehran.ir).

According to the prepared maps and statistical reports presented in the tables, the results of successive years will be compared with each other.

In maps in Fig. 3 and 4, the amount of red color which indicates building class, in most areas in 2019 compared to 2018 has been increased, including the northeastern, western and southern parts of the city, this phenomenon can be observed in two tables which demonstrated 2743.99 (hectares) increment. Fortunately water class and planet class which are essential in a huge city like Tehran have improved for water class 195.91 (hectares) and for planet class 4074.37 (hectares), however in soil class 7014.27 (hectares) decrement can be presentable According to the prepared maps and statistical reports presented in the tables, the results of successive years will be compared with each other.. In maximum likelihood classification for Fig. 4 overall accuracy was 90.2813% & Kappa Coefficient was 0.8343 for 2018 and Overall Accuracy = 90.9924% & Kappa Coefficient = 0.8591 for 2019.

Table 2. Area of four considered Classes in2018

| Object * | Class name | Count | Area (sq m) | Area (hectares) |
|----------|------------|---------|-------------|-----------------|
| 1 | Soil | 3005895 | 300589500 | 30058.95 |
| 2 | Plant | 711817 | 71181700 | 7118.17 |
| 3 | Water | 69318 | 6931800 | 693.18 |
| 4 | Build-up | 3786988 | 378698800 | 37869.88 |

Total area: 75740.18

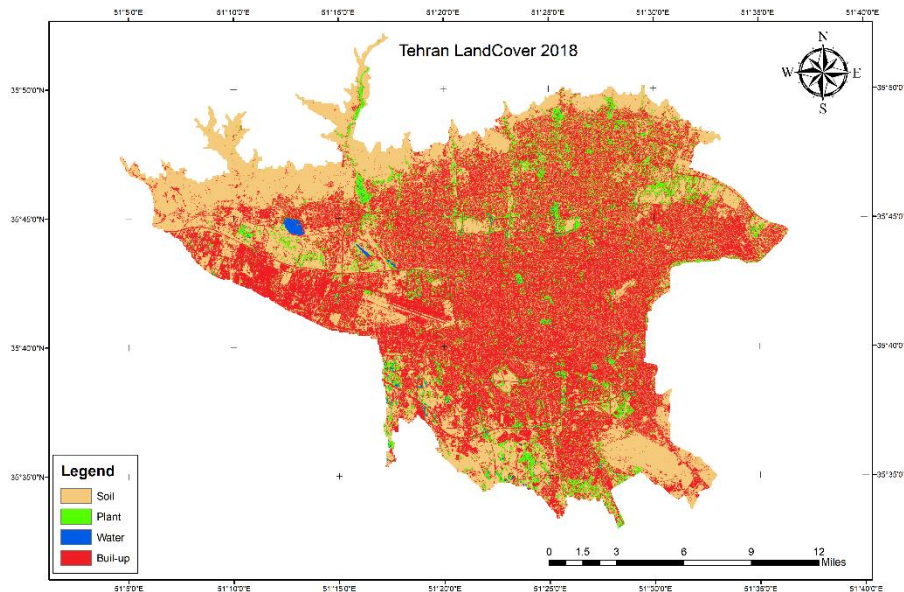


Fig. 3. Tehran representing land cover n 2018

Table 3. Area of four considered classes in 2019

| Object* | Class name | Count | Area(sq m) | Area (hectares) |
|---------|------------|---------|------------|-----------------|
| 1 | Soil | 2304468 | 230446800 | 23044.68 |
| 2 | Plant | 1119254 | 111925400 | 11192.54 |
| 3 | Water | 88909 | 8890900 | 889.09 |
| 4 | Build-up | 4061387 | 406138700 | 40613.87 |

Total area: 75740.1

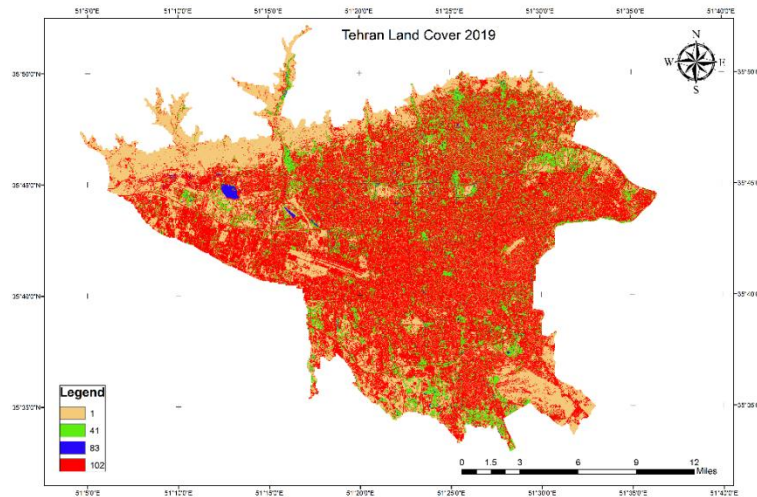


Fig. 4. Tehran Land Use in 2019

Table 4. Area of four considered classes in 2020

| Object * | Class name | Count | Area (sq m) | Area (hectares) |
|----------|------------|---------|-------------|-----------------|
| 1 | Soil | 2568978 | 256897800 | 25689.78 |
| 2 | Plant | 869232 | 86923200 | 8692.32 |
| 3 | Water | 12672 | 1267200 | 126.72 |
| 4 | Build-up | 4123136 | 412313600 | 41231.36 |

Total area: 75740.18

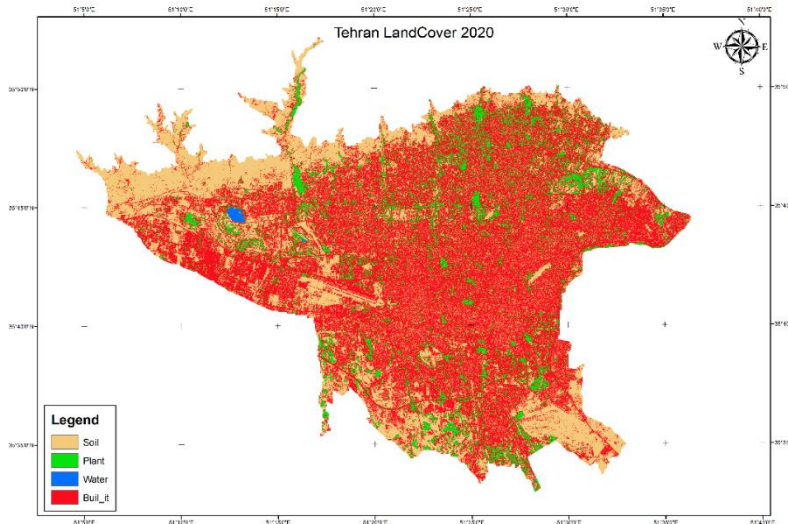


Fig. 5. Tehran representing land cover in 2020

Table 5. Area of four considered classes in 2021

| Object * | Class name | Count | area(sq m) | Area (hectares) |
|----------|------------|---------|------------|-----------------|
| 1 | Soil | 2303267 | 230326700 | 23032.67 |
| 2 | Plant | 1329724 | 132972400 | 13297.24 |
| 3 | Water | 19897 | 1989700 | 198.97 |
| 4 | Build-up | 3921130 | 392113000 | 39211.3 |

Total area: 75740.18

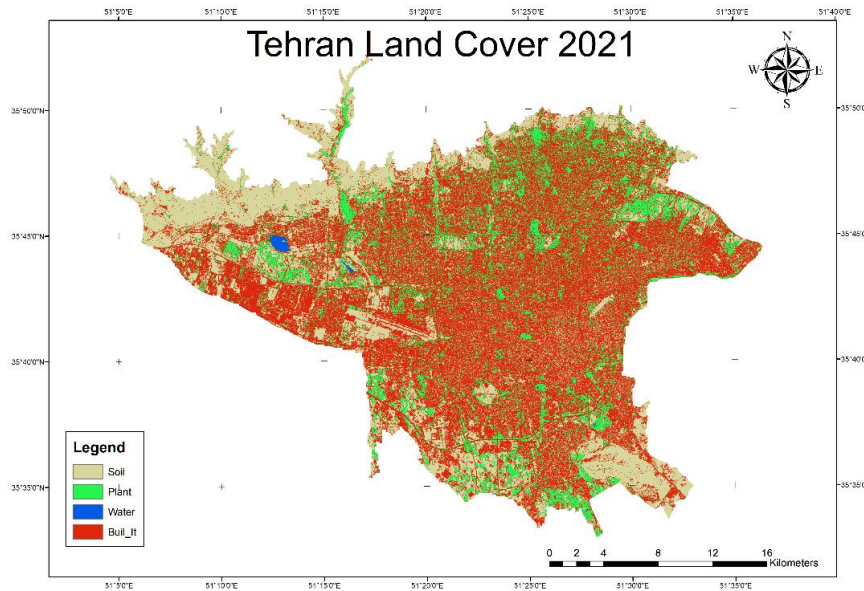


Fig. 6. Tehran representing land cover in 2021

By comparing maps of 2020 to 2019 it can be concluded build-up class continues to expand 617.49 (hectares) trend but unfortunately plant area have a significant drop about 2500.22 (hectares) and it seems that this change and the change of water class 126.72 (hectares) decrement became to barren area which classified by soil name had 2645.09 (hectares) increment compare to 2019, In the classification with Overall Accuracy = 90.8818% & Kappa Coefficient = 0.8560 earned.

Unlike previous results in 2021 earned map build-up class have 2020.06 (hectares) decrement and water class large increased about 72.75 (hectares), also plant class have

increment of 4604.92 (hectares) but soil class decrement was 2657.1 (hectares) compare to 2020 given information. This map produced by Overall Accuracy = 90.9924% & Kappa Coefficient = 0.8591.

Investigation of build-up class as a major reason of this study demonstrated 2080.3 (hectares) expansion and 90.69 (hectares) of increment for water class and soil class also have been expanded 1225.8 (hectares) compare to 2021. these results trend can be shown clearly in graph 1. For this map Overall Accuracy = 93.0685% & Kappa Coefficient = 0.8278 have been earned.

Table 6. Area of four considered classes in 2022

| Object * | Class name | Count | area(sq m) | Area (hectares) |
|----------|------------|---------|------------|-----------------|
| 1 | Soil | 2425847 | 242584700 | 24258.47 |
| 2 | Plant | 993988 | 99398800 | 9939.88 |
| 3 | Water | 24966 | 2496600 | 249.66 |
| 4 | Build-up | 4129217 | 412921700 | 41292.17 |

Total area: 75740.18

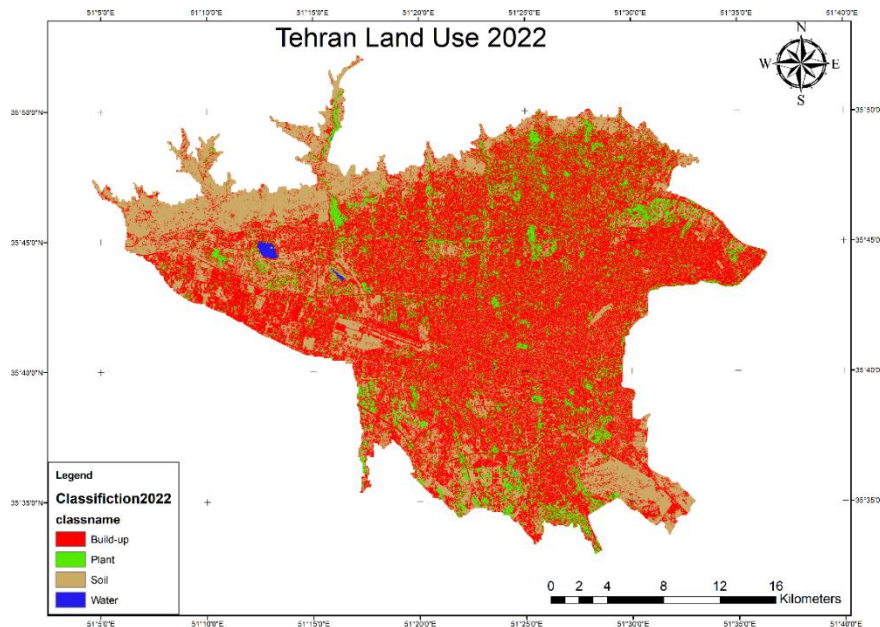
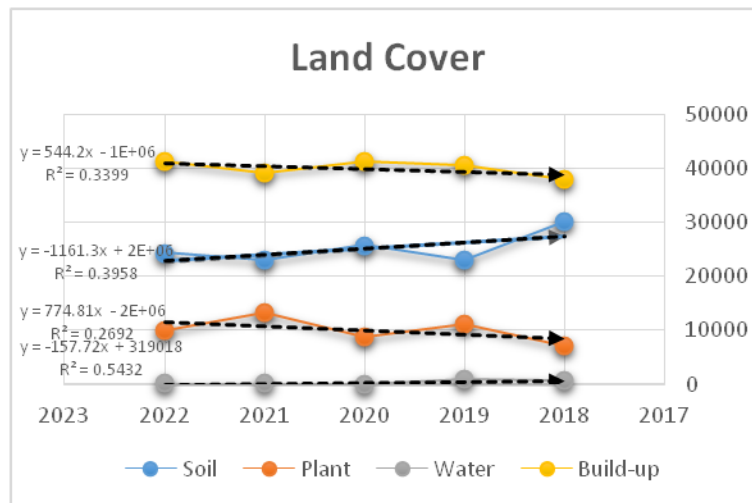


Fig. 7. Tehran representing land cover in 2022



Graph 1. Change of the classes by linear regression

Table 7. Area of each class during study time (hectares)

| (Class name)/Year | Soil | Plant | Water | Build-up |
|-------------------|----------|----------|--------|----------|
| 2018 | 30058.95 | 7118.17 | 693.18 | 37869.88 |
| 2019 | 23044.68 | 11192.54 | 889.09 | 40613.87 |
| 2020 | 25689.78 | 8692.32 | 126.72 | 41231.36 |
| 2021 | 23032.67 | 13297.24 | 198.97 | 39211.3 |
| 2022 | 24258.47 | 9939.88 | 249.66 | 41292.17 |

By considering the fluctuations have been observed, and applying linear regression to predict the trend of increase or decrease for these four main classes it can be concluded that building area with the largest portion of the area

of this city is expanding continuously, on the other hand barren area that we called soil in this study had been decreased extremely fast .water area approximately was dropt but because of having few portion of this city's area drop can't

recognize facility, but in plant class we obtain unstable changes however in 2022 compare to 2018 grow up is obvious.

In this table areas can be compared to whole of study period, as previous results build-up class is expanding during 2018 to 2022 and plant class have increase but the essential class became lower than half in 5 years and it should be consider by managers, and environment maker decisions, barren areas which named soil in this research have obviously decrement.

5. CONCLUSION

The propose of this research was monitoring land cover changes for Tehran city in recent year to forecasting future trends, for this study satellite images downloaded from Copernicus earth data site which provide sentinel images in open access platform, and conventionally appropriate for implement required correction, therefore images downloaded for September which is in summer time in study area. For outperform corrections like geometric, atmospheric and radiometric correction have applied in ENVI5.6 software then classification in ArcGIS Pro with four standard and gave more difference of characteristics in classes soil (barren lands), plant (contain of forest, agricultural and urban green space), build-up (urban , sub-urban ,roads and all human constructive buildings) and water area is done and five distinctive maps produced by reliable accuracy, this part presented that ArcGIS pro can classify faster and facile , results showed that this software with 2 parameter of accuracy ,overall accuracy and acceptable kappa coefficient is applicability for classification. Tables 2-6 demonstrated trend of changes and compared years to years, it is obvious that build-up class had a significant expansion. So, accordingly area of each class changes corresponding to end and first year of study ,whole area soil class have decrease 5800.48 (hectares), and build-up class increased 3422/29 (hectares), plant class (2821.71) increased and water class deceased 443.52 (hectares). The results of study can help decision makers for better management in different fields such water supply, environment protecting, urban development and natural resources and economy.

6. FUTURE CHALLENGES

If the process of increasing urban areas continues at the same speed, the soil areas will

soon become residential areas and it can have harmful consequences for the city of Tehran in terms of urban traffic and air pollution. It was created in 2021 and sudden changes in the size of the classes in the short period of the study period can be considered .Knowing the amount and trend of changes in different applications Monitoring land cover changes using remote sensing it leads to more understanding and making appropriate management decisions in the relationship it will be used in different ways. Of course, it should be acknowledged that the main reason for these changes is the lack of suitable jobs in other areas, which causes people to migrate to Tehran as the capital city is to destroy resources in order to earn income it becomes natural in the region. Therefore, proper management and implementation of the program-Land preparation seems necessary in this area. ArcGIS pro can be used as a faster and accurate tool for satellite data processing in the combination of remote sensing and spatial data.

COMPETING INTERESTS

Authors have declared that no competing interests exist.

REFERENCES

1. Chen X. A simple and effective radiometric correction method to improve landscape change detection across sensors and across time. Remote sensing of Environment. 2005;63-79.
2. Gharagozlou AN. Assessment of physical changes and analysis of urban development using remote sensing with high resolution & GIS/RS(case study: District 5 of Tehran), . Journal of Environmental Science and Technology; 2009.
3. Jensen J. Introductory Digital Image Processing: A Remote Sensing Perspective. Englewood Cliff. NJ: Prentice – Hall. 2005;318.
4. B, SS. (Detecting and Assessing the Spatial-Temporal Land Use Land Cover Changes of Bahrain Island during 1986–2020 Using Remote Sensing and GIS. Earth System and Environment; 2022.
5. Karimi NK. Development and application of an analytical framework for mapping probable illegal dumping sites using nighttime light imagery and various remote

- sensing indices. Waste Management. 2022;143:195-205.
6. Felix II. Locating Suitable Solid Waste Dumping Sites using Remote Sensing and GIS Techniques in Aba Municipal, South-Eastern Nigeria." European Journal of Applied Sciences. European Journal of Applied SCIENCES. 2022;10.2.
 7. Urban Land-Cover Change Detection through Sub-Pixel Imperviousness Mapping Using Remotely Sensed Data. (n.d.).
 8. Norman L, Feller M, Guerin D. Forecasting urban growth across the United States-Mexico border. *Comput. Environ. Urban Syst.* 2009;33:150-159.
 9. Surender Kumar¹ RS. Geospatial Applications in Land Use/Land Cover Change Detection for Sustainable Regional Development: The Case of Central Haryana, India. *Geomatics and Environmental Engineering.* 2021;15. Available:<https://doi.org/10.7494/geom.2021.15.3.81>
 10. Guanyao Xie 1, *. a. Mapping and Monitoring of Land Cover/Land Use (LCLU) Changes in the Crozon Peninsula (Brittany, France) from 2007 to 2018 by Machine Learning Algorithms (Support Vector Machine, Random Forest, and Convolutional Neural Network) and by Post-Classification; 2018.
 11. Wang Z, Yang X, Lu C, Yang F, Wang Z, Yang X, Lu C, Yang F. A scale self-adapting segmentation approach and knowledge transfer for automatically. Updating land use/cover change databases using high spatial resolution images. *Int. J. Appl. Earth Obs, Geoinf.* 2018;69:88–98.
 12. Guan Y, Zhou Y, He B, Liu X, Zhang H, Feng S. Improving Land Cover Change Detection and Classification With BRDF Correction and Spatial Feature Extraction Using Landsat Time Series: A Case of Urbanization in Tianjin, China. *IEEE J. Sel. Top.* 2020;4166-4177.
 13. Mahsa Safaripour, d.n. Monitoring land cover changes using remote sensing and information system. *Environmental Science and TECHNOLOGY*; 2016.
 14. (n.d.). Available: www.irmo.ir.
 15. (n.d.). Available: www.wikipedia.org.
 16. Story M, Congalton R. Accuracy assessment: a user's perspective. *Photogrammetric Engineering and Remote Sensing.* 1986;397-399.
 17. Available: <https://sentinels.copernicus.eu/web/sentinel/user-guides/sentinel-3-olci/resolutions/radiometric>
 18. Richards J. Remote sensing digital image analysis: An introduction. . Springer-Verlag, Berlin, Germany; 1999.
 19. Henry C. (Retrieved 17 November). ESA Awards Sentinel 3C and D Satellite Contracts to Thales Alenia Space. Via Satellite; 2016.
 20. (n.d.). Available:<https://sentinels.copernicus.eu/web/sentinel/user-guides/sentinel-3-olci/resolutions/radiometric>
 21. Scepan J. Thematic validation of high-resolution global land-cover data sets. *Photogrammetric Engineering and Remote Sensing.* 1999;1051-1060. Available: <https://doi.org/10.1007/s41748-022-00315-z>
 22. Rencher AC, Christensen WF. Chapter 10, Multivariate regression – Section 10.1, Introduction", *Methods of Multivariate Analysis, Wiley Series in Probability and Statistics.* 2012;709.
 23. Alavi Panah, e. a. Application of remote sensing in earth science(soil science). Tehran University Press; 2013.
 24. (n.d.). Available:<https://pro.arcgis.com/en/pro-app/latest/get-started/get-started.htm>

© 2023 Vahidi et al.; This is an Open Access article distributed under the terms of the Creative Commons Attribution License (<http://creativecommons.org/licenses/by/4.0>), which permits unrestricted use, distribution, and reproduction in any medium, provided the original work is properly cited.

Peer-review history:
The peer review history for this paper can be accessed here:
<https://www.sdiarticle5.com/review-history/97756>